

# Formation of the pyruvoyl-dependent proline reductase Prd from *Clostridioides difficile* requires the maturation enzyme PrdH

Christian Behlendorf <sup>a</sup>, Maurice Diwo <sup>a</sup>, Meina Neumann-Schaal <sup>b,c</sup>, Manuela Fuchs <sup>d,e</sup>, Dominik Körner <sup>f</sup>, Lothar Jänsch <sup>f</sup>, Franziska Faber <sup>d,e</sup> and Wulf Blankenfeldt <sup>a,c,\*</sup>

<sup>a</sup>Department Structure and Function of Proteins, Helmholtz Centre for Infection Research, 38124 Braunschweig, Germany

<sup>b</sup>Leibniz-Institut DSMZ-Deutsche Sammlung von Mikroorganismen und Zellkulturen GmbH, 38124 Braunschweig, Germany

<sup>c</sup>Institute for Biochemistry, Biotechnology and Bioinformatics, Technische Universität Braunschweig, 38106 Braunschweig, Germany

<sup>d</sup>Helmholtz Centre for Infection Research (HZI), Helmholtz Institute for RNA-based Infection Research (HIRI), 97080 Würzburg, Germany

<sup>e</sup>Faculty of Medicine, Institute for Molecular Infection Biology (IMIB), Julius-Maximilians-University of Würzburg (JMU), 97080 Würzburg, Germany

<sup>f</sup>Cellular Proteomics, Helmholtz Centre for Infection Research, 38124 Braunschweig, Germany

\*To whom correspondence should be addressed: Email: [wulf.blankenfeldt@helmholtz-hzi.de](mailto:wulf.blankenfeldt@helmholtz-hzi.de)

Edited By: Patrick Stover

## Abstract

Stickland fermentation, the coupled oxidation and reduction of amino acid pairs, is a major pathway for obtaining energy in the nosocomial bacterium *Clostridioides difficile*. D-proline is the preferred substrate for the reductive path, making it not only a key component of the general metabolism but also impacting on the expression of the clostridial toxins TcdA and TcdB. D-proline reduction is catalyzed by the proline reductase Prd, which belongs to the pyruvoyl-dependent enzymes. These enzymes are translated as inactive proenzymes and require subsequent processing to install the covalently bound pyruvate. Whereas pyruvoyl formation by intramolecular serinolysis has been studied in unrelated enzymes, details about pyruvoyl generation by cysteinolysis as in Prd are lacking. Here, we show that Prd maturation requires a small dimeric protein that we have named PrdH. PrdH (CD630\_32430) is co-encoded with the PrdA and PrdB subunits of Prd and also found in species producing similar reductases. By producing stable variants of PrdA and PrdB, we demonstrate that PrdH-mediated cleavage and pyruvoyl formation in the PrdA subunit requires PrdB, which can be harnessed to produce active recombinant Prd for subsequent analyses. We further created PrdA- and PrdH-mutants to get insight into the interaction of the components and into the processing reaction itself. Finally, we show that deletion of *prdH* renders *C. difficile* insensitive to proline concentrations in culture media, suggesting that this processing factor is essential for proline utilization. Due to the link between Stickland fermentation and pathogenesis, we suggest PrdH may be an attractive target for drug development.

**Keywords:** proline reductase, pyruvoyl enzyme, autoproteolysis, *Clostridioides difficile*, Stickland metabolism

## Significance Statement

Energy conservation via Stickland fermentation was first described in the 1930s, yet information about the key enzyme of this process, Prd, is scarce, despite the fact that its central role in both metabolism and toxin production make it a promising target for intervention. Here we show how a small, previously overlooked hypothetical protein that we named PrdH mediates formation of the catalytically essential pyruvoyl group of Prd. In vivo studies in *Clostridioides difficile* emphasize the critical importance of PrdH in the utilization of proline. The known interplay between proline reduction and toxin production leads us to suggest PrdH as a potential drug target. Moreover, our findings open the door for further structural and functional studies with recombinantly produced active Prd.

## Introduction

The nosocomial anaerobic gut bacterium *Clostridioides difficile* is a leading cause of healthcare-associated infections and therefore a major burden for healthcare systems worldwide (1). Infection by *C. difficile* is closely linked to its unique metabolism (2), where one of the major processes of energy acquisition involves the

coupled oxidation and reduction of pairs of amino acids in a process known as Stickland fermentation (3). While the oxidation of the first amino acid yields ATP via substrate-level phosphorylation, the second amino acid acts as an electron acceptor for the regeneration of NAD<sup>+</sup>. In addition to ATP generation in the oxidative arm of Stickland fermentation, new evidence suggests that

**Competing Interest:** The authors declare no competing interest.

**Received:** December 29, 2023. **Accepted:** June 9, 2024

© The Author(s) 2024. Published by Oxford University Press on behalf of National Academy of Sciences. This is an Open Access article distributed under the terms of the Creative Commons Attribution-NonCommercial License (<https://creativecommons.org/licenses/by-nc/4.0/>), which permits non-commercial re-use, distribution, and reproduction in any medium, provided the original work is properly cited. For commercial re-use, please contact [reprints@oup.com](mailto:reprints@oup.com) for reprints and translation rights for reprints. All other permissions can be obtained through our RightsLink service via the Permissions link on the article page on our site—for further information please contact [journals.permissions@oup.com](mailto:journals.permissions@oup.com).

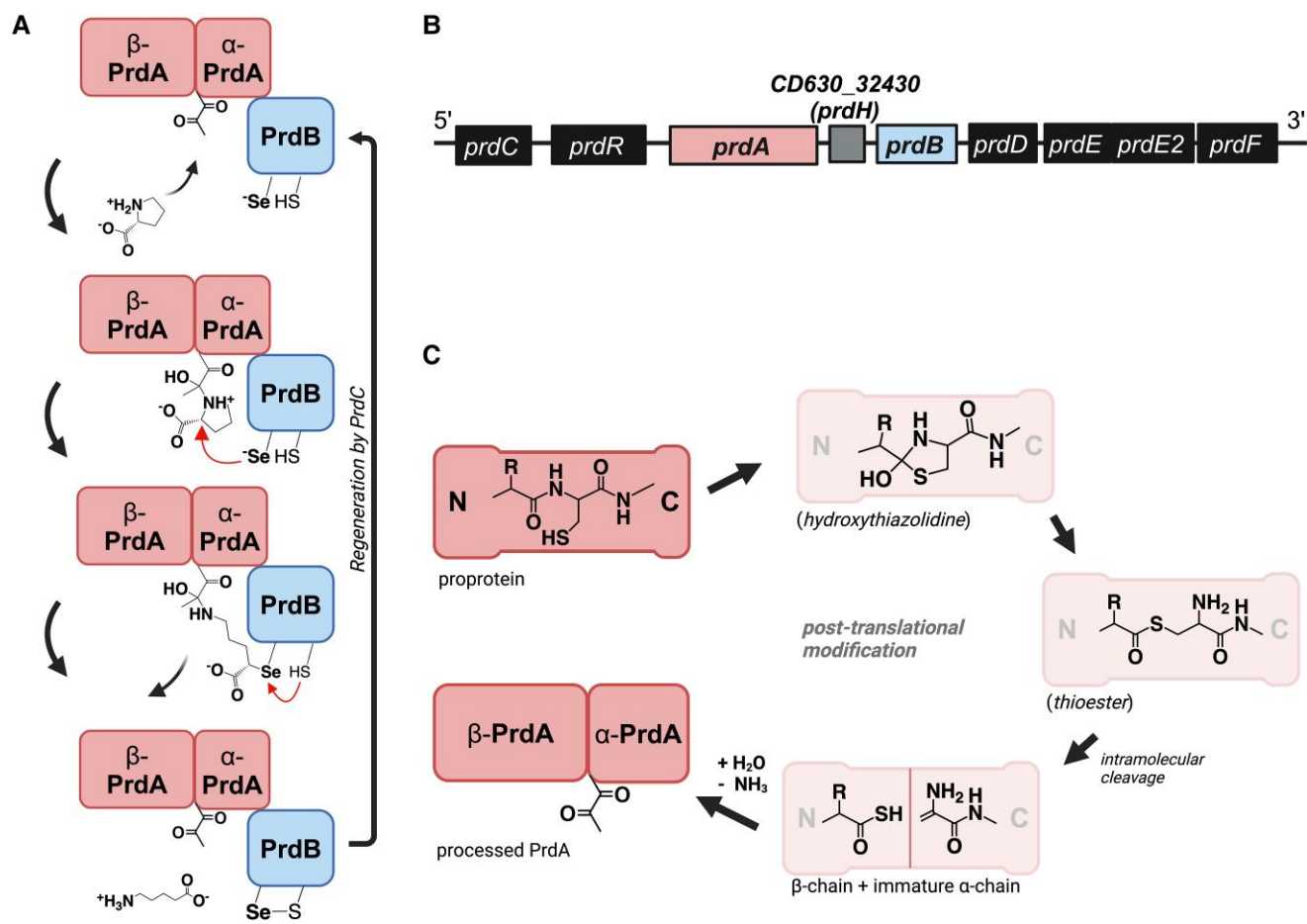


**Fig. 1.** Proline reductase Prd is a pyruvoyl- and selenocysteine-containing enzyme. A) Reduction of D-proline starts with binding the substrate at the pyruvoyl cofactor of the  $\alpha$ -subunit of PrdA. The selenocysteine of PrdB attacks the  $\alpha$ -C-atom of D-proline, which induces ring cleavage and subsequent release of the product 5-aminovalerate. Regeneration of the complex is mediated by the electron transport protein PrdC (5). B) Organization of the *prd*-operon in *Clostridioides difficile*. PrdR regulates the expression of the following genes in response to the cellular D-proline level. PrdA and PrdB encode the two subunits of the proline reductase complex. PrdD and PrdE/E2 share high structural similarities with PrdA, but their function is still unknown. PrdF encodes a proline racemase, catalyzing the conversion of L-proline to D-proline. The enzyme CD630\_32430 (PrdH) catalyzes pyruvoyl cofactor formation in PrdA and is the main focus of this study. C) Proposed mechanism of pyruvoyl cofactor formation in PrdA, based on observations made for pyruvoyl-dependent decarboxylases (7).

the reductive section of the pathway contributes to ATP formation as well, feeding into an electron bifurcation system that ultimately adds to proton motive force. This has recently been demonstrated for the reduction of D-proline in *Clostridioides sporogenes* (4) and seems to explain the preference of D-proline as the reduced substrate (5).

Reduction of D-proline in Stickland fermentation leads to 5-aminovalerate and is catalyzed by the D-proline reductase complex Prd, which belongs to the small but ubiquitous family of pyruvoyl-dependent enzymes (6). In Prd, the pyruvoyl-containing PrdA subunit associates with a second, selenocysteine-containing protein termed PrdB, which is encoded in the same gene cluster. While PrdA and PrdB together are catalytically competent to perform D-proline reduction (Fig. 1A), they assemble into a large multimer of nearly 1 MDa molecular weight, probably representing a (PrdA/PrdB)<sub>10</sub> stoichiometry (8).

A main characteristic of the structurally diverse pyruvoyl-containing enzymes is their translation as inactive proproteins (termed  $\pi$ -unit), which then mature via intramolecular cleavage at a specific sequence position with subsequent formation of a covalently bound pyruvate at the N-terminus of the C-terminal fragment, resulting in an active enzyme. Pyruvoyl-dependent

enzymes can be divided into two classes. The first is represented by decarboxylases, which includes metabolic enzymes such as histidine decarboxylase, S-adenosylmethionine decarboxylase, aspartate decarboxylase, and phosphatidylserine decarboxylase (6). These enzymes consist of two subunits and contain a serine that induces serinolysis at the specific cleavage site of the proprotein. The second class, to which Prd belongs, are reductases that possess a cysteine instead.

For the serine-containing pyruvoyl proenzymes, the intramolecular processing reaction is well-established (9). A related mechanism has also been proposed for the reductases, albeit that these enzymes would employ cysteine to cleave the immature protein as shown in Fig. 1C. Here, the thiol group of the cysteine is predicted to attack the  $\alpha$ -C-atom of the preceding amino acid. A hydroxythiazolidine intermediate is formed and S/N-acyl shift leads to formation of a thioester intermediate.  $\beta$ -Elimination with subsequent addition of water and loss of ammonia leaves covalently bound pyruvate at the N-terminus of the C-terminal fragment, termed the  $\alpha$ -subunit, after cleavage from the  $\beta$ -subunit. Similar to the pyruvoyl-containing decarboxylases, the  $\alpha$ - and  $\beta$ -subunit remain bound to each other in the reductases.

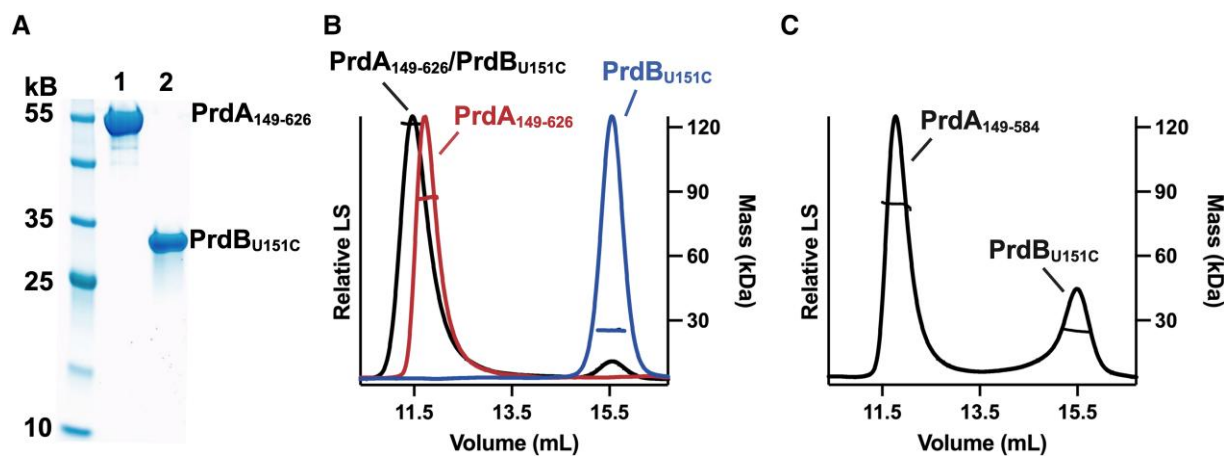


**Fig. 2.** Unprocessed PrdA interacts with PrdB. A) SDS-PAGE analysis of recombinant PrdA<sub>149-626</sub> (1) and PrdB<sub>U151C</sub> (2). B) SEC-MALS results of three independently performed experiments. PrdA<sub>149-626</sub> (eluting at approx. 11.8 mL) elutes with a single peak. The measured mass of ~80 kDa indicates a rapid equilibrium between monomeric and dimeric states. The measured mass of PrdB<sub>U151C</sub> (~24 kDa, eluting at 15.5 mL) is consistent with the calculated mass of the monomer. The mixture of PrdA<sub>149-626</sub> and PrdB<sub>U151C</sub> (eluting at 11.5 mL) results in a shifted elution with a measured mass of ~125 kDa, indicating strong interaction between the two subunits. Similar to PrdA<sub>149-626</sub>, a rapid equilibrium between different oligomeric states is assumed. C) SEC-MALS analysis of a mixture of PrdA<sub>149-584</sub> and PrdB<sub>U151C</sub>. No interaction between the two proteins is observed.

Although the mechanism of pyruvoyl formation is considered to be spontaneous, it has previously not been possible to activate recombinantly expressed PrdA under physiological conditions (10). The enzyme remained in its unprocessed state, leading to the question if an additional factor is needed for the maturation process. Similar observations were made for the histidine decarboxylase (11) and the L-aspartate- $\alpha$ -decarboxylase (12), where such processing factors could indeed be identified.

In this study, we demonstrate that pyruvoyl maturation of the PrdA subunit of Prd is catalyzed by PrdH, a small conserved hypothetical protein co-encoded in the *prd*-operon (Fig. 1B). We further show that pyruvoyl formation requires the presence of PrdB, yielding stable full-length or truncated active Prd. Further experiments with mutants of PrdA and PrdH gave insights into requirements and interaction between assembly and processing reaction of the complex. In order to emphasize the crucial role of PrdH in proline reduction *in vivo*, a knock-out mutant was generated, showing that PrdH is essential for normal growth of *C. difficile* in proline-containing minimal media.

## Results

### Truncation allows recombinant expression of a stable PrdA fragment in *Escherichia coli*

The proline reductase Prd is a multimeric complex with a molecular mass of ~960 kDa (6). Although isolation of this complex from *Clostridioides* has first been performed decades ago (13), recombinant generation of the complete complex has remained unsuccessful due to aggregation and degradation of PrdA (9). To alleviate this problem, we expressed several N-terminally truncated variants of PrdA, finding that omission of the first 148 amino acids led to stable fragments that could be purified with chromatographic methods. Nevertheless, in line with previous studies (6), spontaneous processing to a pyruvoyl-containing protein was not observed. Instead, PrdA<sub>149-626</sub> and similar fragments remained in their un-cleaved state (Figs. 2A and S1).

The second Prd subunit, PrdB, is a selenocysteine-containing protein, requiring the detection of a specific SECIS element in the secondary mRNA structure to recognize the UGA-codon as a signal for incorporation of selenocysteine instead of stopping the

translation process (14). Despite the fact that *E. coli* produces selenocysteine-containing enzymes as well, *E. coli* did not recognize the SECIS element of clostridial mRNA in our experiments. We therefore created a PrdB variant in which we substituted the selenocysteine at position 151 with cysteine. This variant, PrdB<sub>U151C</sub>, has a molecular weight of 25.7 kDa and could readily be isolated using immobilized metal affinity chromatography (IMAC) followed by size exclusion chromatography (SEC, Fig. 2A).

### PrdA<sub>149-626</sub> and PrdB<sub>U151C</sub> interact *in vitro*

The Prd complex is composed of the two subunits of PrdA and of PrdB, suggesting that both proteins may interact tightly. To test whether truncated recombinantly expressed PrdA<sub>149-626</sub> and PrdB<sub>U151C</sub> engage in a complex despite lacking the pyruvoyl functionality in the PrdA subunit, we employed size exclusion chromatography coupled to multiangle light scattering (SEC-MALS). The measured mass for PrdA<sub>149-626</sub> alone was found to lie in between the calculated mass of a monomer and dimer, which may indicate a rapid equilibrium between both the states. PrdB<sub>U151C</sub>, on the other hand, was found to be monomeric. Mixing both subunits at a 1:1 molar ratio before SEC led to co-elution of both proteins, indeed hinting at a strong interaction. The shifted elution peak is consistent with an increased measured molecular weight. A minor fraction of free PrdB<sub>U151C</sub> was also observed. For the mixture of PrdA<sub>149-626</sub> and PrdB<sub>U151C</sub>, the data indicate the formation of heterotetramer (PrdA<sub>149-626</sub>)<sub>2</sub>/(PrdB<sub>U151C</sub>)<sub>2</sub> with an expected molecular weight of 180 kDa, as well as smaller amounts of heterotrimer (PrdA<sub>149-626</sub>)<sub>2</sub>/PrdB<sub>U151C</sub> and heterodimer PrdA<sub>149-626</sub>/PrdB<sub>U151C</sub>, again hinting at a rapid equilibrium that displays an apparent molecular weight of 120 kDa. Larger complexes as observed for native full-length Prd isolated from *C. difficile* (see Complex assembly requires processing section) are missing, suggesting that the N-terminus of PrdA may be crucial for higher order oligomerization (Fig. 2B).

Further, we aimed at investigating PrdA sequence motifs required for complex formation with PrdB. Toward this, we created different N- or C-terminally truncated variants of PrdA and employed SEC-MALS analysis to assess complex formation. This

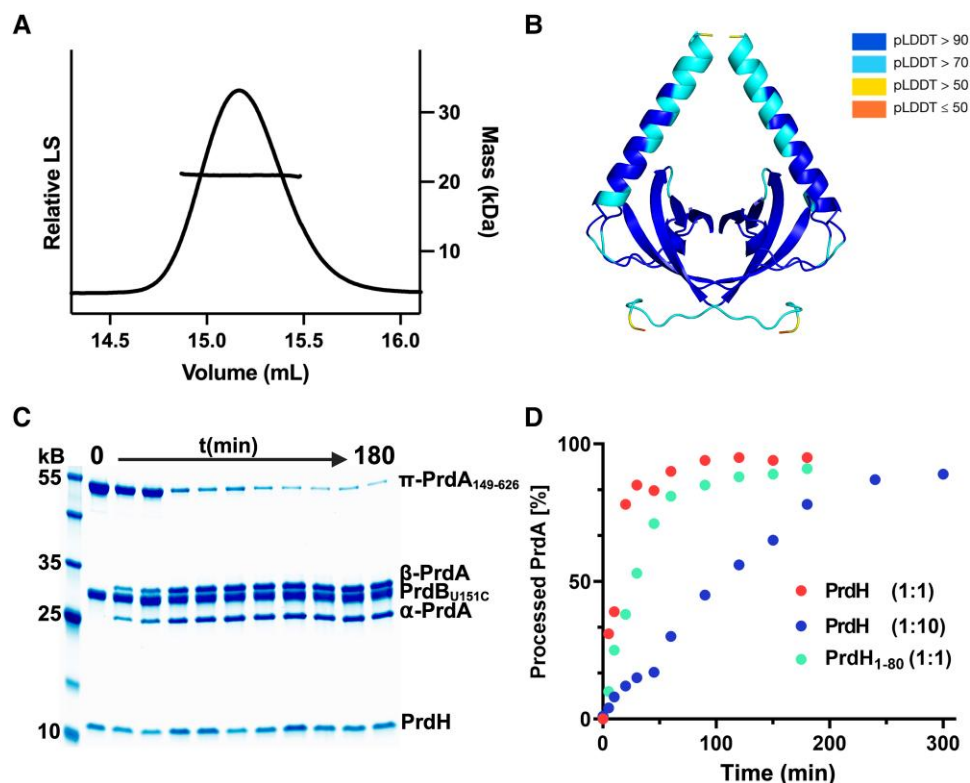


**Fig. 3.** The homodimeric protein PrdH catalyzes cleavage of PrdA in the PrdA/B complex. A) SEC-MALS analysis of recombinant PrdH reveals a dimeric protein. B) The structure of the PrdH dimer as predicted with AlphaFold2 via ColabFold (17). Colors represent the pLDDT confidence score of AlphaFold2 (blue = highly confident, red = poorly confident). The image was created using PyMol (18). C) Time-dependent in vitro processing of  $\pi$ -PrdA fragment PrdA<sub>149-626</sub> in complex with PrdB by PrdH at equimolar ratio. D) Band intensities were measured using ImageJ (19). The amount of processed PrdA is shown.

revealed that a relatively short 26-residue C-terminal segment of PrdA enables interaction with PrdB: while PrdA<sub>149-612</sub> still binds PrdB (Fig. S2), PrdA<sub>149-584</sub> lost this ability completely despite otherwise being stable (Fig. 2C).

### Identification of PrdH (Cd630\_32430) as a conserved protein in the *prd*-operon

The fact that recombinantly expressed PrdA remained unprocessed led us to assume that installation of the pyruvoyl moiety requires additional factors. Therefore, we analyzed the *prd*-operon and found an open reading frame downstream of *prdA*, numbered CD630\_32430, that encodes a hypothetical protein of 94 amino acids (Fig. 1B).

Comparing the genome of *C. difficile* with other proline-reducing bacteria using BLAST and the STRING database (15) shows high conservation of this gene among bacteria harboring the proline reductase (Fig. S3). Available transcriptome data also show transcription of CD630\_32430 in vivo (16). Due to the high conservation, we decided to name the gene *prdH*.

Next, we aimed at isolating PrdH protein for further experiments. The protein was recombinantly expressed in *E. coli*, followed by purification via affinity chromatography and SEC. While the calculated mass of PrdH is ~11 kDa, we observed a molecular weight of ~22 kDa in SEC-MALS analysis (Fig. 3A), demonstrating that PrdH assembles into a homodimer. Because crystallization attempts were not successful, we used AlphaFold2 via ColabFold (17, 20) to construct a structural model of the dimer with a pLDDT > 90 in most regions of the protein (Fig. 3B). The high-confidence score of this model also encouraged us to perform

further structure-based analysis of PrdH (see Assessment of important motifs in PrdH section).

### PrdH mediates cleavage of PrdA but requires the presence of PrdB

The maturation and concomitant installation of the pyruvoyl group in PrdA involves cleavage between T420 and C421. Although this has previously been considered to involve an auto-catalytic process (21), we could not observe spontaneous cleavage in any of the recombinant fragments of PrdA (Figs. 2A and S1), which is in line with previous reports (10). We therefore reasoned that installation of the pyruvoyl group may require the conserved protein PrdH as a processing factor. Incubation of PrdA<sub>149-626</sub> with PrdH indeed led to cleaved protein, but to our surprise, this also required PrdB<sub>U151C</sub>, which needed to be included in equimolar amounts with respect to the PrdA fragment (Fig. 4A). Similar to PrdA<sub>149-626</sub>, the slightly shortened PrdA<sub>164-626</sub> was cleaved in the presence of PrdB<sub>U151C</sub> and PrdH as well (Fig. S4). This suggests that PrdH-mediated processing of PrdA requires prior complex formation with PrdB, which was corroborated by the finding that PrdA<sub>149-584</sub>, which does not interact with PrdB (see PrdA<sub>149-626</sub> and PrdB<sub>U151C</sub> interact in vitro section) was not cleaved in a similar experiment (Fig. 4A).

For further investigation of the cleavage reaction, a time course experiment was performed by stopping the reaction after different intervals, followed by subsequent densitometric analysis of SDS-PAGE bands. This revealed a half-life of approximately 20 min when PrdH was employed at equimolar concentration (Fig. 3C and D). Approximately 95% turnover was achieved after 2 h.

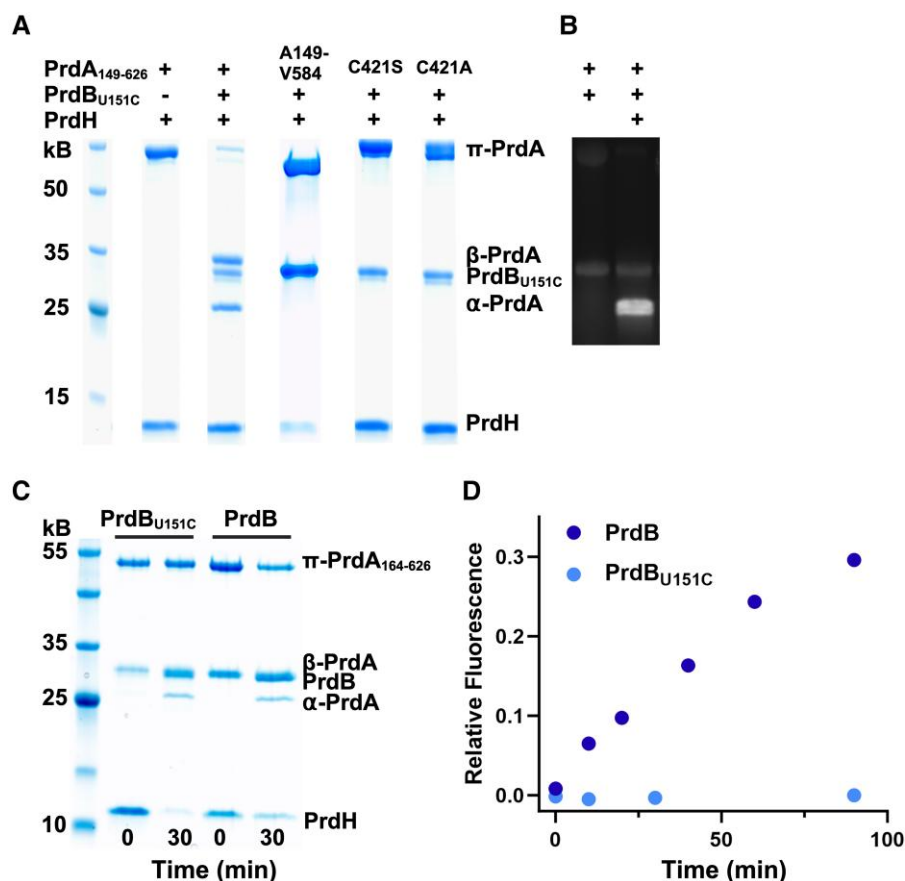


**Fig. 4.** PrdH-mediated cleavage requires PrdB and C421 to install the pyruvoyl moiety in PrdA, allowing the production of catalytically active Prd fragments. A) SDS-PAGE showing the requirement of a preformed PrdA/B complex and of PrdA<sub>C421</sub> for processing. Different mixtures of PrdA<sub>149-626</sub> or its C421 mutants, PrdB<sub>U151C</sub>, and PrdH have been analyzed. B) Detection of the pyruvoyl cofactor in  $\alpha$ -PrdA via fluorescence after incubation with fluorescein thiosemicarbazide. C) Recombinant expression of selenocysteine-containing PrdB leads to the same PrdH-mediated PrdA processing as with PrdB<sub>U151C</sub>. Note that this experiment was performed with PrdA<sub>164-626</sub>, leading to a  $\beta$ -PrdA fragment of nearly identical molecular weight as PrdB (28.6 kDa vs. 27.9 kDa), which explains why these proteins are not separated on the SDS-PAGE. D) Detection of 5-aminovalerate via fluorescence after reaction with *o*-phthalaldehyde demonstrates the proline reductase activity of PrdA<sub>164-626</sub>/PrdB after processing with PrdH.

When PrdH was reduced to 10 mol-%, the half-life of PrdA<sub>149-626</sub> increased to 120 min but led to almost the same amount of turnover, showing that PrdH acts catalytically on the PrdA fragment (Fig. 3D). Given this enzymatic activity, we next investigated if PrdH would also act on variants of PrdA in which the cysteinolysis-mediating C421 has been replaced. Both the alanine mutant PrdA<sub>149-626-C421A</sub> and the serine mutant PrdA<sub>149-626-C421S</sub> were not processed, indicating that cysteine is indeed required for maturation (Fig. 4A).

Next, we tested if the PrdH-mediated cleavage of PrdA indeed leads to formation of the electrophilic pyruvoyl group in the C-terminal fragment. Here, we used fluorescein thiosemicarbazide, which, as a nucleophile, attacks the pyruvoyl group and leads to specific labeling of the PrdA- $\alpha$ -subunit as expected (22) (Fig. 4B). Finally, we assessed if the PrdA- $\beta$ -subunit indeed contains a C-terminal thiocarboxylate group as would be expected after the intramolecular cleavage reaction shown in Fig. 1C. Here, we used the thiocarboxylate detection reagent lissamine rhodamine B sulfonyl azide (LRSA) (23) but could not observe specific labeling of the PrdA- $\beta$ -subunit. Further, we performed electron spray ionization—mass spectrometry (ESI-MS) measurements on intact protein samples (Fig. S5) and mass-spectrometric peptide analysis of protease-treated PrdA<sub>149-626</sub> cleaved in the presence of PrdB<sub>U151C</sub> and PrdH (Fig. S6). Whereas these experiments confirmed the installation

of a pyruvoyl group in  $\alpha$ -PrdA, they suggest that  $\beta$ -PrdA does indeed not contain a C-terminal thiocarboxylate, hinting at a possible hydrolysis reaction subsequent to cleavage of PrdA. This sets  $\beta$ -PrdA apart from other enzymes such as e.g. ThiS-like proteins, where the thiocarboxylate group plays an important functional role as a sulfur donor (23).

### In vitro-processed PrdA in complex with PrdB reduces D-proline

To test whether PrdA reduces D-proline to 5-aminovalerate after PrdH-mediated processing, *o*-phthalaldehyde, which reacts with 5-aminovalerate to form a fluorescent derivate, was used (24). Although the crucial pyruvoyl group could be clearly identified (see PrdH mediates cleavage of PrdA but requires the presence of PrdB section), PrdA<sub>164-626</sub>/PrdB<sub>U151C</sub> was not capable of catalyzing the reaction (Fig. 4D). We hypothesized that the selenocysteine to cysteine substitution at U151 not only reduced but also completely impeded the activity of PrdB. To circumvent difficulties of expressing selenocysteine-containing proteins in *E. coli* (see Truncation allows recombinant expression of a stable PrdA fragment in *E. coli* section), we used amber suppression tRNA to incorporate selenocysteine into PrdB (25). Purification of PrdB was identical to PrdB<sub>U151C</sub> and incubation with PrdA<sub>164-626</sub> and

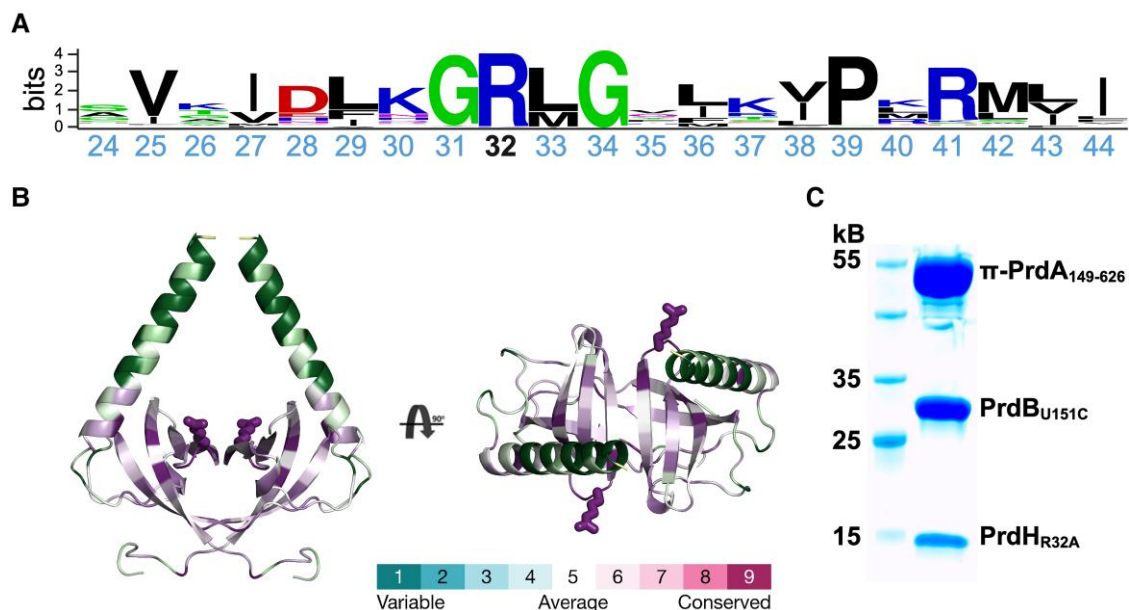


**Fig. 5.** Identification of important motifs in PrdH. A) Sequence conservation within a central stretch of PrdH, based on the alignment of 198 sequences (created with WebLogo (26)). B) Sequence conservation mapped onto the AlphaFold2-model of PrdH (created with ConSurf (27)). Note the high conservation of the exposed residue R32. C) SDS-PAGE analysis shows the requirement of R32 for PrdH-mediated processing of PrdA.

PrdH possessed similar processing of the PrdA fragment (Fig. 4C). The resulting processed PrdA<sub>164-626</sub>/PrdB complex indeed reduced D-proline to 5-aminovalerate (Fig. 4D), showing that PrdH-mediated processing of the PrdA/PrdB complex is the only requirement to generate an enzymatically active proline reductase. Further oligomerization to the large multimeric complex found in *C. difficile*, which apparently depends on motifs contained within the first 148 amino acids of PrdA (see PrdA<sub>149-626</sub> and PrdB<sub>U151C</sub> interact in vitro section), is, on the other hand, not essential for reductase activity.

### Assessment of important motifs in PrdH

The fact that AlphaFold2 generates a high-confidence structural model of the PrdH dimer together with the availability of sequences from nearly 200 PrdH homologs provided an opportunity for the assessment of important sequence and structure motifs in PrdH.

First, we noted that *C. difficile* PrdH is predicted to possess a conspicuously long 25-residue  $\alpha$ -helix at its C-terminus, which could be envisioned as a structural element that interacts with PrdA, in particular because both PrdA and PrdH are homodimeric proteins. However, this helix is not conserved in PrdH homologs of several other bacteria (Fig. 5B), and indeed, shortening this  $\alpha$ -helix by 14 residues did not affect recombinant production of the protein, and the resulting variant was not strongly impaired in catalyzing the processing of PrdA (Fig. 3D).

On the other hand, analysis of PrdH homologs identifies R32 as the most highly conserved residue in these proteins (Fig. 5A). Further, according to the predicted model, R32 is located at an exposed position on the surface (Fig. 5B). Indeed, substituting R32 with alanine through site-directed mutagenesis abrogated the activity of PrdH completely, corroborating its importance (Fig. 5C). Further experiments will be required to gain more detailed insight into the molecular mechanism underlying PrdH-mediated pyruvoyl installation into PrdA.

### Pull-down assays reveal dynamics of the PrdA/B/H interaction

We have established that processing of PrdA requires both complex formation with PrdB and the enzymatic activity of PrdH (see PrdH mediates cleavage of PrdA but requires the presence of PrdB section). Therefore, at a certain time, all three components should form a ternary complex. For further investigation, pull-down experiments using SEC were performed in which all three proteins were expressed separately and mixed at equimolar ratios directly before performing SEC to avoid any prior processing of  $\pi$ -PrdA (Fig. 6). First, PrdH co-eluted with PrdA<sub>149-626</sub>, indicating interaction between these two proteins, although the processing reaction requires PrdB as well (see PrdH mediates cleavage of PrdA but requires the presence of PrdB section). The main elution peak of a mixture of PrdA<sub>149-626</sub>, PrdB<sub>U151C</sub>, and PrdH suggests interaction between all three components, with the processing reaction occurring during the chromatography run. A mixture of PrdA<sub>149-626\_C421S</sub>, PrdB<sub>U151C</sub>, and PrdH shows similar co-elution, but no processing product is observed, indicating that PrdH indeed interacts with the PrdA/B complex, but because the C421S-substitution in PrdA<sub>149-626</sub> abolishes the processing reaction, its release from the PrdA/B complex is blocked. Finally, mixing PrdA<sub>149-626</sub>, PrdB<sub>U151C</sub>, and PrdH<sub>R32A</sub> revealed no interaction of the PrdH-mutant with the complex at all, indicating that the highly conserved R32 plays a crucial role for the interaction.

### Complex assembly requires processing

The experiments summarized in the previous sections were performed with N-terminally truncated variants of PrdA, which was necessary to avoid aggregation and degradation observed when full length PrdA was produced alone in *E. coli* (Truncation allows recombinant expression of a stable PrdA fragment in *E. coli* section). To our surprise, however, recombinant expression of full length PrdA became feasible through coexpression with PrdB and PrdH. Here, SEC-MALS analysis of the purified recombinant Prd reveals the same molecular mass as for native protein purified

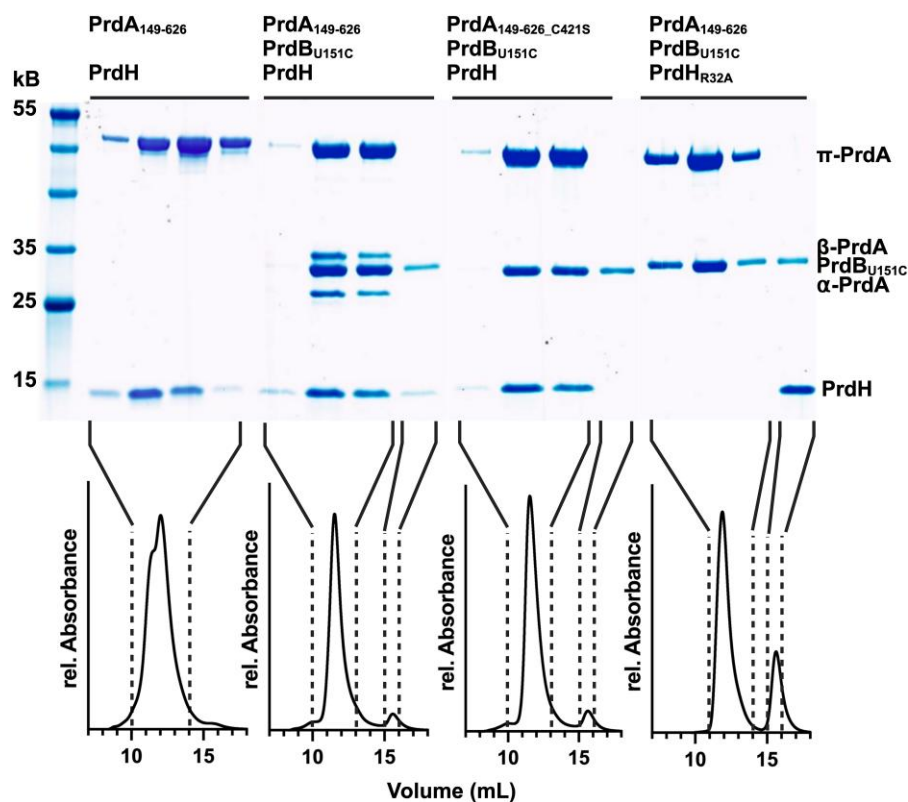


**Fig. 6.** PrdA, PrdB, and PrdH engage in different complexes during pyruvoyl formation. SEC profiles of recombinant proteins mixed directly before analysis were recorded to identify complexes that form during the maturation of Prd. From left to right: PrdH co-eluted with PrdA<sub>149-626</sub>, indicating interaction between these two proteins in the absence of PrdB. Co-elution of PrdA<sub>149-626</sub>, PrdB<sub>U151C</sub> and PrdH suggests interaction between all three components, with the processing reaction occurring during the chromatography run. While C421S-substitution in PrdA<sub>149-626</sub> abolishes the processing reaction, co-elution suggests that the interaction with PrdB<sub>U151C</sub> and PrdH still prevails. Mixing PrdA<sub>149-626</sub>, PrdB<sub>U151C</sub>, and PrdH<sub>R32A</sub> shows that the PrdH-mutant does not interact with the complex unprocessed PrdA and PrdB at all, pointing at the critical role of R32. Note that monomeric PrdB and the homodimeric PrdH have similar molecular weight, leading to co-elution without complex formation.

from *C. difficile*, namely approx. 960 kDa, indicating a (PrdA/PrdB)<sub>10</sub> stoichiometry (Figs. 7 and S7). This not only shows that formation of the decameric Prd complex requires PrdH-mediated processing of the PrdA chain but also provides opportunities for further analysis of the complete enzyme.

### The $\Delta$ prdH mutant of *C. difficile* is insensitive to D-proline

To determine the importance of PrdH in vivo, we created an in-frame deletion of *prdH* in *C. difficile* 630 ( $\Delta$ prdH) via homologous recombination (28), to preserve expression of the remaining *prd* operon. Growth of the  $\Delta$ prdH and the isogenic wild-type (WT) strains was assessed in *C. difficile* minimal medium (CDMM), which was supplemented with L-proline at concentrations ranging from 0 to 8 g/L (Fig. 8). In line with previous studies (5, 29, 30), *C. difficile* WT displayed proline-dependent growth, leading to higher cell density at higher proline levels. In contrast, the growth of the  $\Delta$ prdH-mutant was found to not respond to proline. Surprisingly and against first intuition, the mutant showed similar growth rates as the WT strain at the highest proline concentrations, irrespective of the amount of L-proline present in the medium. A similar observation was made in a recent study using a PrdB-knockout, where the switching to alternative energy metabolism-associated pathways with concomitant sufficient internal proline generation for protein biosynthesis otherwise consumed by Prd were assumed as the basis for the observed phenotype (29). Our new

data suggest that PrdH is another essential factor for the formation of active Prd and hence for proline-dependent growth.

## Discussion

Proline reductase Prd is a key enzyme of Stickland fermentation, a process that utilizes the coupled oxidation and reduction of amino acids for energy generation in bacteria such as *C. difficile*. Prd is a large multimeric enzyme consisting of PrdA and PrdB chains that contain an essential selenocysteine in PrdB and require the posttranslational installation of a pyruvoyl group via internal cysteinolysis in the PrdA subunits. While pyruvoyl moieties are also found in other unrelated proteins, details of pyruvoyl maturation in PrdA are not understood.

In this study, we show that the conserved open reading frame CD630\_32430, renamed here as *prdH*, encodes for a homodimeric 92-residue-containing protein with crucial function for pyruvoyl formation in Prd. Using recombinant proteins, we further demonstrate that PrdA needs to undergo complex formation with PrdB before PrdH-mediated processing can occur. These findings allow the drawing of conclusions about the maturation process of the native proline reductase complex: after the translation of PrdA as an inactive proprotein, it has to interact with the separately translated PrdB first before PrdH can induce self-mediated cleavage of PrdA with concomitant pyruvoyl group formation. In this regard, the requirement of PrdB binding could be a mechanism to prevent the maturation of free PrdA, since the pyruvoyl group

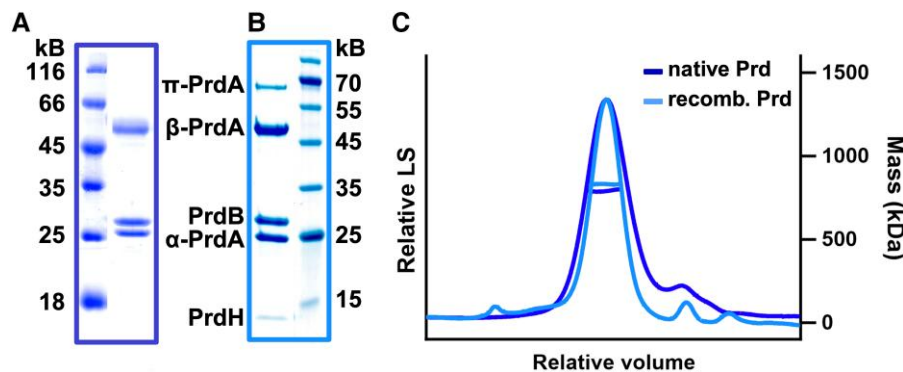


**Fig. 7.** Coexpression of PrdA, PrdB, and PrdH in *E. coli* leads to Prd with similar properties as Prd isolated from *C. difficile*. A) Prd purified from *C. difficile* 630 $\Delta$ erm (see also Fig. S7). B) Prd generated by coexpression of PrdA, PrdB<sub>U151</sub>, and PrdH in *E. coli*. Small amounts of  $\pi$ -PrdA and PrdH were copurified with Prd, indicating incomplete processing. Note that different molecular weight markers and SDS-PAGE were used in (A) and (B), leading to slightly different apparent molecular weights. C) Comparison of SEC-MALS profiles of natively and recombinantly expressed Prd reveals similar molecular masses.

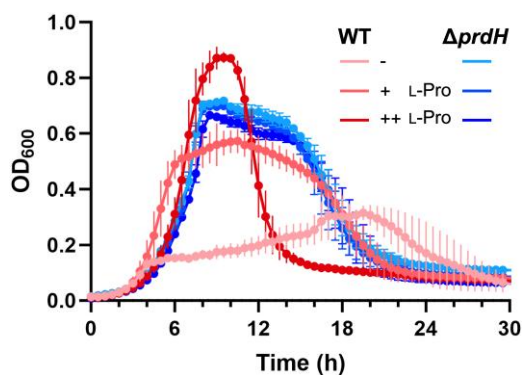


**Fig. 8.** The  $\Delta$ prdH variant of *C. difficile* is insensitive to the L-proline concentration in growth media. Both *C. difficile* 630 (WT) and *C. difficile* ( $\Delta$ prdH) were grown anaerobically in CDMM medium under anaerobic conditions supplemented with different concentrations of L-proline (+ L-Pro: 2 g/L; ++ L-Pro: 8 g/L). Data points represent the means of quadruplicate cultures with error bars representing standard deviations.

of such a protein would be expected to be highly reactive towards nucleophiles, leading to unspecific and potentially dangerous reactions before active D-proline-specific Prd is formed. On the other hand, our experiments with soluble fragments of PrdA show that higher order oligomerization to the 960 kDa complex, which is apparently mediated through the first 148 amino acids of PrdA, is not required to generate processed Prd subunits. Through processing of PrdA<sub>164-626</sub> and incorporation of Sec into PrdB, we could further show that oligomerization is not essential for proline reductase activity, since the nonoligomerized processed protein consisting of a (PrdA<sub>164-626</sub>)<sub>2</sub>PrdB<sub>2</sub> heterotetramer was fully functional in reducing D-proline to 5-aminovalerate.

Further, our findings indicate that PrdH catalyzes the processing reaction, i.e. PrdH is an enzyme. However, since the pyruvoyl installation is an intramolecular reaction conceptually not requiring catalysis by an external factor, it is at present not clear how PrdH stimulates this reaction mechanistically. Future studies will reveal if complex formation induces strain in the amino acid sequence undergoing cysteinolysis in PrdA or if PrdH participates in the reaction by e.g. acting as an acid/base catalyst. However, our finding that PrdH already interacts with PrdA in the absence of PrdB, albeit that PrdB is nonetheless required for pyruvoyl formation, suggests that PrdH and PrdB may act together in increasing conformational strain in PrdA. Such conformational strain seems to be a general

requirement to induce acyl shift reactions in proteins (31), a common feature shared by diverse autoprocessing mechanisms such as protein splicing or cleavage of hedgehog protein precursors (21).

Interestingly, the PrdA<sub>149-626\_C421S</sub> mutant shows no processing at all, while complex formation with PrdB and PrdH was unaffected. In contrast, processed PrdA<sub>149-626</sub> shows no interaction with PrdH. PrdH only interacts with unprocessed PrdA and detaches from the complex as soon as the reaction is complete. This is a prerequisite for PrdH's ability to act as an enzyme.

The overall findings lead us to assume that PrdH is an essential enzyme for proline reduction in *C. difficile*. Since *C. difficile* produces higher levels of CDI-inducing toxins at low proline concentrations (30), which hints at the physiological importance of Stickland fermentation in the context of virulence, PrdH may be an attractive target for pharmaceutical intervention.

The observed insensitivity and hence nonphysiological behavior of the constructed PrdH-knockout-mutant to L-proline in the growth medium confirmed this hypothesis. Further, it could be shown that the processing reaction is a prerequisite for complex assembly, allowing the stable isolation of recombinantly expressed full length Prd. This opens opportunities for further structural and functional studies of Prd, which are currently pursued in our group.

## Materials and methods

### Bacterial strains and growth media

Genes were amplified from genomic DNA of *C. difficile*  $\Delta$ 630 (DSM 27543). For purification of native Prd, *C. difficile* 630 $\Delta$ erm (DSM 28645) was used. Both strains were obtained from the DSMZ culture collection. Cloning and expression work was performed in *E. coli*. For cloning, either NEB Turbo Competent *E. coli* (High Efficiency) or Top10 (Invitrogen) were used. For expression, *E. coli* BL21 (DE3) or One Shot BL21 Star (DE3) was used. Overnight cultures were grown in LB-medium. For protein expression, ZYM-5052 autoinduction medium (32) was used. Depending on the plasmid, either 100 mg/L ampicillin or 30 mg/L (100 mg/L for expression) kanamycin was added. *Clostridioides difficile* cultures were grown anaerobically inside a Coy chamber (85% N<sub>2</sub>, 10% H<sub>2</sub>, 5% CO<sub>2</sub>) in Brain Heart Infusion (BHI) broth or on BHI agar plates (1.5% agar). When required, 15 mg/L thiamphenicol, 250 mg/L cycloserine, or 8 mg/L cefoxitin were added. For growth in defined CDMM, medium was prepared as described by Neumann-Schaal et al. (33) with minor alterations: NaH<sub>2</sub>PO<sub>4</sub> was added to a final concentration of 16.7 mM and HNaO<sub>3</sub>Se to

a final concentration of 9.9  $\mu\text{M}$ . Subcultures of four replicates were used for inoculation of main cultures with CDMM, supplemented with different concentrations of L-proline. Growth was measured using a Synergy H1 microplate reader.

## Plasmids

All plasmids used in this study are listed in Table S1. Cloning for recombinant expression was performed via classical restriction and ligation or with the SLIC method (34) by employing the ClonExpress Ultra One Step Cloning Kit from Vazyme (Cat#C115). Site-directed mutagenesis was performed with the QuikChange protocol. The required oligonucleotide primers for all molecular biology procedures are listed in Table S2. The resulting plasmids are pET19b or pET15b-based and encoded for single N- or C-terminally 6xHis-tagged proteins, with the exception of a pACYCDuet-1-derived coexpression vector, where N-terminally StrepII-tagged PrdB<sub>U151C</sub> was ligated into multiple cloning site 1 and full-length PrdA in multiple cloning site 2. All affinity tags are cleavable by Tobacco Etch Virus (TEV) protease. Amino acid sequences of the resulting proteins are listed in Table S3.

## Protein expression and purification

Plasmid-transformed *E. coli* were grown in LB-medium at 37 °C and 130 rpm overnight. The overnight culture was used to inoculate 1 L ZYM-5052 media, supplemented with 100 mg/L ampicillin or 100 mg/L kanamycin (pET-based vectors) and 34 mg/L chloramphenicol (pACYCDuet-1) as required, to an OD<sub>600</sub> of 0.1. The cells initially were grown at 37 °C and 130 rpm for 3 h and then for another 25 h at 20 °C before harvesting by centrifugation and storing at -80 °C until further preparation.

For protein purification, the cells were resuspended in 50 mM HEPES, 300 mM NaCl, 2.5% glycerol, pH 7.5 with protease inhibitors (cOmplete mini EDTA-free, Sigma Aldrich) followed by lysis through sonication and subsequent centrifugation at 100,000 g for 45 min. The supernatant was then applied to either Ni<sup>2+</sup>-charged HisTrap HP 5 mL (Cytiva) or StrepTrap HP 5 mL (Cytiva) via an ÄKTA pure or ÄKTA go system (Cytiva). Elution of bound protein was performed using elution buffer (20 mM HEPES, 300 mM NaCl, 2.5% glycerol, pH 7.5 and either 1 mM des-thiobiotin for StrepII-tagged protein or 250 mM imidazole for His-tagged protein). 6xHis-tags were removed during overnight dialysis with 6xHis-tagged TEV protease, followed by another pass over the IMAC column to remove uncleaved protein and TEV protease. Affinity tags were not removed in experiments with PrdB (Figs. 2–6), PrdA<sub>149-626-C421</sub> mutants (Fig. 4B), the PrdH<sub>R32A</sub> variant (Fig. 5C) and recombinant full-length Prd (Fig. 7). Next, fractions containing pure protein as indicated by SDS-PAGE were concentrated by ultrafiltration and applied to a HiLoad 16/600 Superdex 200 (for PrdA and PrdB) or HiLoad 16/600 Superdex 75 (for CD630\_32430/PrdH) (both Cytiva) equilibrated in SEC buffer (20 mM HEPES, 300 mM NaCl, 2.5% glycerol, pH 7.5). Fractions containing the desired pure protein as indicated by SDS-PAGE were pooled, concentrated, frozen in liquid nitrogen and stored at -80 °C for further analysis.

Native Prd was isolated by modification of a previously published protocol (35). *Clostridioides difficile* 630 $\Delta$ erm (DSM 28645) was cultivated anaerobically in L-proline-containing CDMM (0.76 g/L consisting of 0.1 g/L added to the 0.66 g/L of the casamino acids as characterized for this casamino acids lot, Merck) and harvested by centrifugation in the late exponential phase. The pellet of 1.6 L cell culture was resuspended in 40 mL lysis buffer (50 mM HEPES pH 8, 500 mM NaCl, 10 mM imidazole, 5 mM BME, DNase I,

cOmplete EDTA-free protease inhibitor cocktail) and cells were lysed by sonication before slow addition of 40 mL ice-cold 2 M (NH<sub>4</sub>)<sub>2</sub>SO<sub>4</sub>. Cell debris and precipitated proteins were separated by centrifugation at 100,000 $\times$ g for 1 h. Prd was then purified from the supernatant as shown in Fig. S7 by hydrophobic interaction chromatography (5 mL HiTrap Butyl HP, Cytiva), followed by an anion exchange step (8 mL MonoQ, Cytiva) and finally SEC (Superose 6 10/30 increase column, Cytiva).

## Size exclusion chromatography—multiangle light scattering

Superdex 200 Increase 10/300 or Superdex 75 Increase 10/300 (both Cytiva) columns were used with an Agilent 1260 Infinity II HPLC system coupled to a miniDAWN TREOS MALS detector and an Optilab T-rEX refractometer (Wyatt Technology Corp.). Degassed SEC buffer (20 mM HEPES, 300 mM NaCl, 2.5% glycerol, pH 7.5) was used for equilibration and 100  $\mu\text{g}$  protein were applied.

## Assay of in vitro cleavage of PrdA

Recombinantly expressed and purified variants of PrdA and PrdB were mixed in small PCR tubes before PrdH was added. All components were present at equimolar concentration. The mixture was incubated at 37 °C for up to 3 h. The reaction was stopped by addition of SDS loading buffer followed by heating at 95 °C for 5 min before applying samples to an SDS gel. For further analysis of the reaction kinetics, band intensities were measured with ImageJ (19).

## Detection of the pyruvoyl cofactor

For detection of the pyruvoyl group, fluorescein thiosemicarbazide was used (22). Five microliter of protein solution (1 mg/mL) were incubated with 10  $\mu\text{L}$  of 300 mM potassium acetate pH 4.6 and 1  $\mu\text{L}$  of 0.1% fluorescein thiosemicarbazide in dimethylsulfoxide for 2 h at room temperature in the dark. Separation of the proteins as well as separation of unbound fluorophore was performed via SDS-PAGE. The N-terminal carbonyl group was identified by detecting the fluorescence on a phosphorimager (Fujifilm FLA-9000).

## Analysis of the C-terminus of $\beta$ -PrdA

To assess the presence of a thiocarboxylate group at the C-terminus at  $\beta$ -PrdA, we synthesized the thiocarboxylate detection reagent LRSA and followed the published protocol (23) to label and SDS-PAGE-purify samples of recombinant full-length Prd as well as PrdA<sub>149-626</sub> before and after processing with PrdB<sub>U151C</sub>/PrdH. However, as no specific labeling could be observed, samples were also analyzed by ESI-MS (Fig. S5) and mass-spectrometric peptide analysis (Fig. S6).

ESI-MS experiments were performed in the positive detection mode of a Bruker maXis HD UHR-TOF mass spectrometer equipped with an Apollo II electrospray source and coupled to a Dionex/Thermo Ultimate3000RS UHPLC- system (column: YMC Accura Triart Bio C4, 100  $\times$  4.6 mm; solvent A: water with 0.1% formic acid (FA), solvent B: acetonitrile with 0.1% FA; 15-min gradient from 1 to 100% buffer B at a flowrate of 0.9 mL/min).

For proteomic analysis, proteins were dissolved in 50 mM TEAB, reduced for 1 h at 56 °C with 5 mM TCEP and alkylated for 30 min at room temperature with 10 mM MMTS. Asp-N (Roche, 0.05  $\mu\text{g}$  to 1  $\mu\text{g}$  protein) was incubated overnight at 37 °C while shaking at 800 rpm. Peptides were then vacuum-dried and resuspended in 50  $\mu\text{L}$  0.1% FA, followed by desalting (C18 ZipTip, Merck), followed by another vacuum drying step and resuspension in 50  $\mu\text{L}$  0.1% FA. LC-MS/MS data were measured on a Dionex Ultimate 3000 n-RSLC system (Thermo Fisher Scientific), linked to an Orbitrap

Fusion Tribrid system mass spectrometer (Thermo Fisher Scientific). Two hundred nanogram peptide sample were loaded on a C18 precolumn (3  $\mu\text{m}$  RP18 beads, Acclaim, 0.075  $\times$  20 mm), washed for 3 min at a flow rate of 6  $\mu\text{L}/\text{min}$ , and separated on a 2  $\mu\text{m}$  C18 analytical column (Pharmafluidics) at a flow rate of 300 nL/min via a linear 30 min gradient from 96.3% MS buffer A (0.1% FA, 5% DMSO) to 31.3% MS buffer B (0.1% FA, 5% DMSO, 80% ACN), followed by a 10 min gradient from 31.3% MS buffer B to 62.5% MS buffer B, followed by a 2 min gradient from 62.5% MS buffer B to 90% MS buffer B. The LC-MS/MS system was operated with Thermo Scientific SII software embedded in the Xcalibur software suite (version 4.3.73.11, Thermo Fisher Scientific). The effluent was electro-sprayed by a stainless-steel emitter (Thermo Fisher Scientific). The mass spectrometer was operated in the “top speed” mode, allowing the automatic selection of as many doubly and triply charged peptides as possible in a 3 s time window, and the subsequent fragmentation of these peptides. Peptide fragmentation was carried out using the higher energy collisional dissociation mode and peptides were measured in the ion trap (HCD/IT). MS/MS raw data files were processed via Peaks Studio 11.0 mediated searches against the  $\beta$ -PrdA sequence. The following search parameters were used: enzyme, asp-n; maximum missed cleavages, 3; fixed modification,  $\beta$ -methylthiolation (C,  $\Delta m = 45.98$  Da); variable modification, oxidation (M,  $\Delta m = 15.99$  Da), Prd\_A\_sulfur (T,  $\Delta m = 15.99$  Da); precursor mass tolerance, 15 ppm; fragment mass tolerance, 0.5 Da. The false discovery rate was set to 1. Peptide spectra were manually checked for correct PrdA sequences and possible modifications.

### Detection of D-proline reduction

For detection of D-proline reduction, a fluorometric assay with o-phthalaldehyde as described by Seto (24) was performed. The mixture for D-proline reduction included 170  $\mu\text{M}$  processed protein in 50 mM HEPES pH 7.5, 150 mM NaCl, supplemented with 10 mM  $\text{MgCl}_2$ , 20 mM DTT, and 10 mM D-proline. The reaction was stopped adding o-phthalaldehyde mixture, which reacts with 5-aminovalerate, building a highly fluorescent derivative. Fluorescence was measured using 340 nm for excitation and 455 nm for emission via Spark Multimode Microplate Reader (Tecan Group Ltd.).

### Generation of a Cd630\_32430 deletion strain

Allelic exchange cassettes were designed with approximately 1.2 kb of homology to the chromosomal sequence flanking the deletion sites of CD630\_32430 and cloned into pJAK112 (Table S1). To avoid affecting transcription and translation of genes located upstream, the deleted region was restricted to 36 nt upstream of the CDS and 177 nt of the CDS. The resulting plasmid (pFF-418) was conjugated into *C. difficile* using *E. coli* CA434 (36) as donor strain according to Kirk et al. (37). Following successful conjugation, mutants were generated according to Fuchs et al. (38). PCR-based screening for the first recombination event was achieved using FFO-1627/-361, FFO-1628/-360, and FFO-1627/-1628 (Table S2). PCR-based screening for the second recombination event was achieved using FFO-1623/-1624 (Table S2).

### Acknowledgments

We thank Ute Widow (Department Structure and Function of Proteins, Helmholtz Centre for Infection Research) and Ulrike Beutling (Department Chemical Biology, Helmholtz Centre for Infection Research) for measuring ESI-MS data. C.B. and M.D.

were supported by the German Research Foundation (DFG GRK 2223: Protein Complex Assembly (PROCOMPAS)). Figures were created with [BioRender.com](https://www.biorender.com).

### Supplementary Material

Supplementary material is available at PNAS Nexus online.

### Funding

This research was supported by the German Research Foundation (DFG GRK 2223: Protein Complex Assembly (PROCOMPAS)).

### Author Contributions

C.B., M.D., M.N.S., M.F., D.K., L.J., and F.F. performed the research. C.B. and W.B. conceived the study and wrote the manuscript.

### Preprint

This manuscript has been posted on the bioRxiv preprint server with DOI 10.1101/2023.12.15.571967 under a Creative Commons license (CC BY-NC-ND).

### Data Availability

Raw data were generated at the Helmholtz Centre for Infection Research (Germany), the Leibniz Institute DSMZ (Germany), and the Julius-Maximilians-University of Würzburg. Derived data supporting the findings of this study are included in the manuscript and/or supporting information.

### References

- 1 Finn E, Andersson FL, Madin-Warburton M. 2021. Burden of *Clostridioides difficile* infection (CDI)—a systematic review of the epidemiology of primary and recurrent CDI. *BMC Infect Dis.* 21: 456.
- 2 Neumann-Schaal M, Jahn D, Schmidt-Hohagen K. 2019. Metabolism the difficile way: the key to the success of the pathogen *Clostridioides difficile*. *Front Microbiol.* 10:219.
- 3 Stickland LH. 1934. Studies in the metabolism of the strict anaerobes (genus *Clostridium*). *Biochem J.* 28:1746–1759.
- 4 Liu Y, et al. 2022. *Clostridium* sporogenes uses reductive Stickland metabolism in the gut to generate ATP and produce circulating metabolites. *Nat Microbiol.* 7:695–706.
- 5 Bouillaud L, Self WT, Sonenshein AL. 2013. Proline-dependent regulation of *Clostridium difficile* stickland metabolism. *J Bacteriol.* 195:844–854.
- 6 Poelje PDV, Snell EE. 1990. Pyruvoyl-dependent enzymes. *Annu Rev Biochem.* 59:29–59.
- 7 Davidson VL. 2020. Protein-derived cofactors. In: Hung-Wen (Ben) L, Begley TP, editors. *Comprehensive natural products III*. Amsterdam, Netherlands: Elsevier. p. 40–574.
- 8 Diwo M. 2021. Towards structure elucidation of the proline reductase complex from *Clostridioides difficile* [PhD dissertation]. Braunschweig, Germany: Technische Universität Braunschweig.
- 9 Davidson VL. 2018. Protein-derived cofactors revisited: empowering amino acid residues with new functions. *Biochemistry.* 57: 3115–3125.
- 10 Bednarski B, Andreesen JR, Pich A. 2001. In vitro processing of the propeptides GrdE of protein B of glycine reductase and PrdA of D-proline reductase from *Clostridium sticklandii*: formation of a

- pyruvoyl group from a cysteine residue. *Eur J Biochem.* 268: 3538–3544.
- 11 Trip H, Mulder NL, Rattray FP, Lolkema JS. 2011. HdcB, a novel enzyme catalysing maturation of pyruvoyl-dependent histidine decarboxylase. *Mol Microbiol.* 79:861–871.
  - 12 Nozaki S, Webb ME, Niki H. 2012. An activator for pyruvoyl-dependent L-aspartate  $\alpha$ -decarboxylase is conserved in a small group of the  $\gamma$ -proteobacteria including *Escherichia coli*. *Microbiologyopen.* 1:298–310.
  - 13 Seto B, Stadtman TC. 1976. Purification and properties of proline reductase from *Clostridium sticklandii*. *J Biol Chem.* 251:2435–2439.
  - 14 Wells M, Basu P, Stolz JF. 2021. The physiology and evolution of microbial selenium metabolism. *Metallomics.* 13:mfab024.
  - 15 Szklarczyk D, et al. 2019. String v11: protein-protein association networks with increased coverage, supporting functional discovery in genome-wide experimental datasets. *Nucleic Acids Res.* 47: D607–D613.
  - 16 Janoir C, et al. 2013. Adaptive strategies and pathogenesis of *Clostridium difficile* from in vivo transcriptomics. *Infect Immun.* 81:3757–3769.
  - 17 Mirdita M, Schütze K, Moriwaki Y, Heo L, Ovchinnikov S, et al. 2022. ColabFold: making protein folding accessible to all. *Nature Methods.* 19:679–682.
  - 18 Schrödinger LLC. *The PyMOL molecular graphics system, version 3.0.*
  - 19 Schneider CA, Rasband WS, Eliceiri KW. 2012. NIH Image to ImageJ: 25 years of image analysis. *Nat Methods.* 9:671–675.
  - 20 Jumper J, et al. 2021. Highly accurate protein structure prediction with AlphaFold. *Nature.* 596:583–589.
  - 21 Paulus H. 2000. Protein splicing and related forms of protein autoprocessing. *Annu Rev Biochem.* 69:447–496.
  - 22 Ahn B, Rhee SG, Stadtman ER. 1987. Use of fluorescein hydrazide and fluorescein thiosemicarbazide reagents for the fluorometric determination of protein carbonyl groups and for the detection of oxidized protein on polyacrylamide gels. *Anal Biochem.* 161: 245–257.
  - 23 Krishnamoorthy K, Begley TP. 2010. Reagent for the detection of protein thiocarboxylates in the bacterial proteome: lissamine rhodamine B sulfonyl azide. *J Am Chem Soc.* 132:11608–11612.
  - 24 Seto B. 1979. Proline reductase: a sensitive fluorometric assay with o-phthalaldehyde. *Anal Biochem.* 95:44–47.
  - 25 Chung CZ, Miller C, Söll D, Krahn N. 2021. Introducing selenocysteine into recombinant proteins in *Escherichia coli*. *Current Protocols.* 1:e54.
  - 26 Crooks GE, Hon G, Chandonia J-M, Brenner SE. 2004. Weblogo: a sequence logo generator. *Genome Res.* 14:1188–1190.
  - 27 Yariv B, et al. 2023. Using evolutionary data to make sense of macromolecules with a “face-lifted” ConSurf. *Protein Sci.* 32: e4582.
  - 28 Cartman ST, Kelly ML, Heeg D, Heap JT, Minton NP. 2012. Precise manipulation of the *Clostridium difficile* chromosome reveals a lack of association between the *tcdC* genotype and toxin production. *Appl Environ Microbiol.* 78:4683–4690.
  - 29 Johnstone MA, Self WT. 2022. D-proline reductase underlies proline-dependent growth of *Clostridioides difficile*. *J Bacteriol.* 204:e0022922.
  - 30 Cersosimo LM, et al. 2023. Central in vivo mechanisms by which *C. difficile*'s proline reductase drives efficient metabolism, growth, and toxin production. bioRxiv 2023.05.19.541423. <https://doi.org/10.1101/2023.05.19.541423>, preprint: not peer reviewed.
  - 31 Johansson DGA, et al. 2009. Protein autoproteolysis: conformational strain linked to the rate of peptide cleavage by the pH dependence of the N  $\rightarrow$  O acyl shift reaction. *J Am Chem Soc.* 131: 9475–9477.
  - 32 Studier FW. 2005. Protein production by auto-induction in high-density shaking cultures. *Protein Expr Purif.* 41:207–234.
  - 33 Neumann-Schaal M, Hofmann JD, Will SE, Schomburg D. 2015. Time-resolved amino acid uptake of *Clostridium difficile* 630 $\Delta$ erm and concomitant fermentation product and toxin formation. *BMC Microbiol.* 15:1–12.
  - 34 Li MZ, Elledge SJ. 2007. Harnessing homologous recombination in vitro to generate recombinant DNA via SLIC. *Nat Methods.* 4: 251–256.
  - 35 Kabisch UC, et al. 1999. Identification of D-proline reductase from *Clostridium sticklandii* as a selenoenzyme and indications for a catalytically active pyruvoyl group derived from a cysteine residue by cleavage of a proprotein. *J Biol Chem.* 274:8445–8454.
  - 36 Woods C, et al. 2019. A novel conjugal donor strain for improved DNA transfer into *Clostridium* spp. *Anaerobe.* 59:184–191.
  - 37 Kirk JA, Fagan RP. 2016. Heat shock increases conjugation efficiency in *Clostridium difficile*. *Anaerobe.* 42:1–5.
  - 38 Fuchs M, et al. 2021. An RNA-centric global view of *Clostridioides difficile* reveals broad activity of Hfq in a clinically important gram-positive bacterium. *Proc Natl Acad Sci U S A.* 118: e2103579118.